Published in final edited form as:
Neuron. 2011 September 8; 71(5): 898–910. doi:10.1016/j.neuron.2011.07.027.

Single units in the medial prefrontal cortex with anxiety-related firing patterns are preferentially influenced by ventral hippocampal activity

Avishek Adhikari[1], **Mihir A. Topiwala**[2], and **Joshua A. Gordon**[2,3]

[1]Department of Biological Sciences, Columbia University, New York, NY, 10032

[2]Department of Psychiatry, Columbia University, New York, NY, 10032

[3]The New York State Psychiatric Institute, New York, NY 10032

SUMMARY

The medial prefrontal cortex (mPFC) and ventral hippocampus (vHPC) functionally interact during innate anxiety tasks. To explore the consequences of this interaction, we examined task-related firing of single units from the mPFC of mice exploring standard and modified versions of the elevated plus maze (EPM), an innate anxiety paradigm. Hippocampal local field potentials (LFPs) were simultaneously monitored. The population of mPFC units distinguished between safe and aversive locations within the maze, regardless of the nature of the anxiogenic stimulus. Strikingly, mPFC units with stronger task-related activity were more strongly coupled to theta-frequency activity in the vHPC LFP. Lastly, task-related activity was inversely correlated with behavioral measures of anxiety. These results clarify the role of the vHPC-mPFC circuit in innate anxiety, and underscore how specific inputs may be involved in the generation of behaviorally relevant neural activity within the mPFC.

INTRODUCTION

The medial prefrontal cortex (mPFC) has been implicated in the regulation and expression of defensive behaviors in rodents, including learned fear and its extinction (Burgos-Robles et al., 2007) as well as innate anxiety (Deacon et al., 2003; Lacroix et al., 2000; Shah et al., 2004; Shah and Treit, 2003, 2004)). Our prior work has suggested that during the expression of innate anxiety, the mPFC works in concert with a major input source, the ventral hippocampus (vHPC) (Adhikari et al., 2010b). Whether and how neural activity in the mPFC relates to anxiety-like behavior is unclear. During cognitive tasks, single unit recordings in the mPFC have task-related firing patterns (Gemmell et al., 2002; Jones and Wilson, 2005; Jung et al., 1998; Pratt and Mizumori, 2001; Sigurdsson et al., 2010a) as well as functional interactions with the hippocampus (Jones and Wilson, 2005; Siapas et al.,

Send correspondence to: Joshua A. Gordon, Department of Psychiatry, Columbia University, 1051 Riverside Drive, Unit 87, Kolb Annex Room L174, New York, NY 10032, Phone: 212 543-6768, Fax: 212 543-1174, jg343@columbia.edu.

AUTHOR CONTRIBUTIONS

A.A. designed and performed the experiments, conducted the data analysis and wrote the paper. M.A.T. assisted in performing the experiments and did the histology. J.A.G. designed the experiments, supervised the performance of the experiments and data analysis, and wrote the paper.

2005; Sigurdsson et al., 2010a; Taxidis et al., 2010). However, it is unknown if mPFC activity is modulated by anxiety-related task features. Furthermore, the relationship between task-related firing patterns and functional coupling with the hippocampus is unclear.

The elevated plus maze (EPM) is an extensively studied test of innate anxiety in rodents (Hogg, 1996). The EPM is conducted in a plus-shaped maze with four arms, two of which are enclosed by high walls and two of which are left open. Wild-type mice generally make fewer entries into and spend less time exploring the aversive open arms, compared to the relatively safe closed arms. Both the mPFC (Gonzalez et al., 2000; Shah and Treit, 2004) and vHPC (Bannerman et al., 2002; Bannerman et al., 2004; Kjelstrup et al., 2002) have been shown to be required for normal anxiety-related behaviors in the EPM. The monosynaptic unidirectional projection from the vHPC to the mPFC (Parent et al., 2009; Verwer et al., 1997) suggests the possibility that these two areas may be part of a functional circuit involved in anxiety-related behavior. Consisent with this notion, we recently found that theta-frequency (4–12 Hz) synchrony between the mPFC and the vHPC tracked and predicted anxiety-related behavior in the EPM (Adhikari et al., 2010b).

These findings lead to following hypotheses: that mPFC neurons represent the anxiety-related features of the EPM; that this representation arises due to input from the vHPC; and that this representation is used by the animal to guide anxiety-related behavior in the maze. To test these hypotheses, we recorded mPFC single units and vHPC local field potentials from mice during exploration of standard and modified EPMs. We found that a majority of mPFC single units had anxiety-related firing patterns in the EPM, regardless of the geometric arrangement of the arms or the stimulus used to induce aversion. Units with more robust paradigm-related activity were more strongly modulated by vHPC theta-frequency activity, indicating their participation in a functional network involving both structures. Lastly, and somewhat counter-intuitively, animals with higher avoidance of the aversive open arms of the EPM had fewer mPFC units with paradigm-related activity, as well as overall higher firing rates compared to mice that displayed lower avoidance. These results underscore how specific inputs may be involved in the generation of behaviorally relevant neural activity within the mPFC, and refine our understanding of the role of the vHPC-mPFC circuit in EPM behavior.

RESULTS

mPFC single units have task-related firing patterns in the standard EPM

To characterize the activity of mPFC single units in the EPM, 79 well-isolated cortical single units were recorded from the deep layers of the prelimbic cortex in 17 129/SvevTac mice during exploration of a standard cross-shaped EPM under dim (200 Lux) illumination. The mean firing rate of these units was 2.05 ± 0.64 Hz. Units with fewer than 100 spikes (n = 10) were excluded from further analysis. Spatial firing maps revealed that many of the single units tended to fire in specific subcompartments of the EPM (Figure 1A–C). For example, the unit shown in Figure 1A fired preferentially in the two closed, or “safe” arms, while the unit in Figure 1B fired preferentially in the two open, or “aversive” arms.

To further characterize firing patterns across the entire population of recorded mPFC units, normalized firing rates (% difference from mean firing rate) were calculated in the five compartments (each open arm; each closed arm; and the center) of the EPM (Figure 2B&C). Units with task-related firing patterns would be expected to have similar firing rates in arms of the same type (open/safe vs. closed/aversive), and negatively correlated firing rates in arms of opposite type. In line with this prediction, firing rates in both closed arms ($r=+0.38$, $p<0.0001$, Figure 2D) and both open arms ($r=+0.25$, $p<0.04$, Figure 2E) were positively correlated, while firing rates across arms of different types were inversely correlated (r=

−0.64 $p<0.0001$, Figure 2F). Note that with the presence of a center compartment, the inverse correlation between arms of different types is not an automatic consequence of the normalization technique (Figure S1).

Negative correlations between one open and one closed arm were present after only 90 seconds of exploration of the EPM ($r=-0.47$, $p<0.001$), demonstrating that single unit representations of EPM arms arise quickly and do not require extensive exploration of the maze. The results were not due to novelty, as similar results were found during a second exposure to the EPM 24 hours later (Figure 3A–B). Moreover, the results were not due to differences in locomotion between the open and closed arms, as velocity and acceleration profiles were similar across arms (Figure 3C–D), and firing rates did not correlate with either measure ($r^2=0.03$, $p=0.6$ for velocity and $r^2=0.02$, $p>0.72$ for acceleration).

Correlations of firing rates between different arms indicate that the population of mPFC single units is capable of representing anxiety-related task components. However, such correlations do not quantify the extent to which the firing pattern of any given single unit is paradigm-related. To address this issue, we first binned each spike train into three-second segments, and calculated the influence of arm type (open vs. closed) on firing rate by ANOVA. 29/69 (42%) of the recorded neurons fired significantly differently ($p<0.05$) to the closed and open arms by ANOVA. Next, to confirm that the observed frequency of task-related firing patterns in the population of single units was not due to chance, an EPM score was calculated for each unit. The EPM score is a normalized ratio of the average difference in firing rates across arms of the same type, compared to the average differences in firing rates across arms of different types (see Experimental Procedures). The resultant measure, which varies from −1 to 1, indicates the degree to which that unit's firing pattern represents the "open vs. closed" structure of the EPM. Units with positive EPM scores closer to 1 represent this structure well; units with EPM scores near or below zero fire do not. Accordingly, the correlation of firing rates across arms of the same type was higher in units with positive EPM scores than in units with negative EPM scores (Figure 4A–B). Furthermore, single units with a significant effect of arm type on firing in the ANOVA had higher EPM scores than other units (mean score =0.3±0.06 and 0.064 ±0.04 for units with and without significant main effects of arm type), demonstrating the utility of the EPM score as a quantification of the strength of paradigm-related activity.

We next examined whether the distribution of EPM scores obtained in our sample (Figure 4C) could have been obtained by chance, using a bootstrap method. Briefly, 500 simulated spike trains were generated for each unit. The location of each spike was assigned randomly from the actual path of the animal in the maze when that spike was recorded, and EPM scores were computed from these simulated spike trains. The distribution of simulated EPM scores (Figure 4C, red line) was significantly different from the experimental distribution ($p<0.0001$, Wilcoxon's rank-sum test), due to the presence of a greater fraction of units with positive (i.e., paradigm-related) EPM scores in the experimental distribution. These results confirm that the paradigm-related firing patterns seen in our sample in the standard EPM were unlikely to have arisen by chance.

mPFC unit firing changes prior to leaving or entering the closed arms

In cognitive tasks, mPFC unit activity predicts future choice behavior (Fujisawa et al., 2008; Peters et al., 2005; Rich and Shapiro, 2009). To examine whether this predictive capacity is seen in during anxiety-related behavior, peri-event time histograms were calculated for each unit across 10-second segments centered at transitions in which the animal exited or entered a closed arm (Figure 5). Binned firing rates were then converted to z-scores and averaged across all cells with positive EPM scores units and all such transitions. As expected, units that fired preferentially in the closed arms had higher firing rates prior to leaving the closed

arm (Figure 5C, upper panel). Consistent with predictive firing patterns, closed arm preferring unit firing rates began to decrease approximately 2.5 seconds before the mouse left the closed arm. Similarly, firing rates of open arm-preferring units were low in the closed arms, and began to increase several seconds before the transition point (Figure 5C, middle panel). During transitions back to the closed arms, firing rates of these neurons demonstrated complementary profiles (Figure 5D). In both types of transitions, units with negative (non-paradigm-related) EPM scores did not display consistent changes in firing rates.

To quantitatively demonstrate predictivity, the time bins at which firing rates began to change were identified using a change point analysis (Gallistel et al., 2004). This method identifies the point at which the slope of the cumulative sum of the time series of interest changes significantly (Kolmogorov-Smirnov test, $p<0.01$). The identified change points are indicated by arrows in Figure 5C–D. Note that in each case, mPFC single unit activity began to change 1.5–2.7s prior to the exit from or entry into the closed arm, demonstrating that firing rates are not simply passively reflecting the location of the animal but rather foreshadowing behavior a few seconds into the future.

To confirm these firing patterns using an unbiased approach, we used principal component analysis (Chapin, 2004) on firing rates of all units during arm transitions (Figure 5E–F). As predicted from the firing patterns described above, the first principal component (PC1) during each transition type appeared to closely follow the patterns of closed- and open-arm preferring units, with PC1 value switching sign at or just prior to the transition point. Closed arm- and open arm-preferring units loaded inversely onto the PC1 for each transition type.

Firing patterns do not depend on arm location or specific sensory cues

The above data demonstrate that mPFC single units fired differently in closed and open arms of the EPM. However, firing patterns shown in Figure 1 could be induced by differences between the closed and open arms that are unrelated to anxiety. One such confound is the geometric arrangement of the arms. It is possible, for example, that a cell that is active preferentially in the open arms is actually firing not because the animal is in the open arms, but rather, because it is walking in the north-south direction. To exclude this possibility, 18 single units were recorded from five additional mice while they explored an altered EPM in which the open arms were adjacent to each other rather than across from each other (Figure 6). Similarly to the results obtained in the standard EPM, firing rates in the altered EPM were positively correlated between arms of the same type (Figure 6B and C, respectively, for the closed arms ($r=+0.71$, $p<0.0003$) and for the open arms ($r=+0.67$, $p<0.001$). Furthermore, firing rates between closed and open arms were negatively correlated, as in the standard EPM ($r= -0.54$, $p<0.002$). To examine the relationship of firing across the two mazes, the same units were recorded while mice were exposed to a standard EPM after a 1-hour delay. Strikingly, firing rates between arms of the same type were positively correlated across the two configurations (Figure 6D–E, $r=+0.43$, $p<0.04$ for the closed arms and $r= +0.53$, $p<0.01$ for the open arms, $n=18$ units). The correlations between firing across the two mazes show that individual mPFC neurons follow arm type (open vs. closed) as opposed to arm location.

A second potential confound is the sensory experience used to induce avoidance. We reasoned that if the firing patterns of mPFC units are indeed associated with anxiety, units should differentiate between safe and aversive arms regardless of the particular anxiogenic cues used. To this end, we characterized the response of mPFC single units to openness and brightness, as both are anxiogenic, despite providing different sensory input. Anxiety induced by openness was studied in a standard EPM with two open and two closed arms, in the dark (closed/open maze). Reponses to anxiety caused by brightness were explored in an

EPM with four closed arms, where two arms were brightly lit (dark/bright maze). These behavioral paradigms were both anxiogenic, as mice avoided the aversive (open or bright) arms in both conditions (% time spent in open arms and bright arms was 21.4 ± 5.3 and 20.3 ± 2.5, respectively, n = 5 naive mice; see Figure 7I).

An additional 8 implanted mice were exposed to both modified mazes. 105 single units were recorded in both mazes. As in the standard EPM, normalized firing rates were inversely correlated between aversive (bright or open) and safe (dark or closed) arms in each maze ($r = -0.51$, $p<0.001$ for closed/open and $r = -0.55$, $p<0.001$ for dark/bright correlations; Figure 7E–F), demonstrating that under these conditions, mPFC neurons continue to represent the task-related features of the mazes. Crucially, firing rates in the aversive (open and dark) arms in the closed/open maze correlated with rates in the aversive (closed and bright) arms in the dark/bright maze ($r=0.21$, $p<0.05$; Figure 7H), even though completely different stimuli were used to induce aversion. The positive correlation between firing rates on arms made aversive through the use of different anxiogenic cues argue strongly that that mPFC single units represent the anxiety-related features of the maze, rather than appearance or configuration of the arms.

Anxiety-related firing patterns are associated with vHPC input

The above results suggest that the mPFC may encode aspects of the environment related to anxiety. We reasoned that since the vHPC and mPFC are required for and synchronize during anxiety (Adhikari et al., 2010b), mPFC single units with more robust anxiety-related firing patterns might be more strongly influenced by vHPC activity. Indeed, EPM scores were higher in units significantly phase-locked to vHPC theta (Rayleigh's $p<0.05$) compared to other units (Figure 8C, mean score = 0.31 ± 0.07 and 0.17 ± 0.04, for phase-locked and other units, respectively, $p<0.05$, n=69 units). Importantly, this result is not due to differences in firing rates, as EPM scores and phase-locking to vHPC theta were correlated, even when phase-locking values were calculated on a subsample of 100 spikes from each unit ($r=+0.25$, $p<0.03$; Figure S2). These results demonstrate that cells that receive vHPC input have stronger anxiety-related firing patterns. Consistent with previous results (Adhikari et al., 2010b), this effect was specific for the theta-frequency range, as EPM scores did not differ with phase-locking to vHPC delta- (1–4 Hz) or gamma-frequency (30–80 Hz) oscillations (data not shown). Furthermore, phase locking of mPFC single units to dHPC theta oscillations was not related to EPM scores (Figure 8D), in agreement with lesion (Kjelstrup et al., 2002) and physiology (Adhikari et al., 2010b) studies suggesting that the dHPC is not required for normal anxiety-related behavior in the EPM.

The above results suggest that mPFC single units with robust anxiety-related firing patterns are preferentially recruited into a circuit involving the vHPC. The projection from the vHPC to the mPFC is unidirectional (Parent et al., 2009; Verwer et al., 1997), and hippocampal theta-range activity has been shown to lead the mPFC (Adhikari et al., 2010a; Siapas et al., 2005; Sigurdsson et al., 2010a). We reasoned that if the vHPC input plays a role in the generation of anxiety-related firing patterns, mPFC single units that follow vHPC theta should have stronger paradigm-related firing patterns compared to units that do not. To find which cells follow hippocampal theta activity, MRL values were calculated after shifting the spike train of each mPFC single unit in time, relative to the vHPC theta-filtered LFP (see Experimental Procedures). Consistent with the known anatomy and previous results, the overall mean lag for maximal phase-locking was negative, indicating that on average, mPFC unit activity followed vHPC activity (mean lag = −13.8 ± 8.1 ms). However, units with positive lags relative to hippocampal theta were also found, similarly to previous reports (Adhikari et al., 2010b; Siapas et al., 2005; Sigurdsson et al., 2010a). Positive lag units may result from chance, or may be involved in polysynaptic modulating of hippocampal activity. Consistent with our prediction, cells that followed the vHPC had significantly higher EPM

scores than other units (Figure 9D, mean score = 0.24 ± 0.047 and 0.07 ± 0.05 for units that follow vHPC theta and other units, $p<0.05$, Wilcoxon's test), consistent with the notion that information from the vHPC plays a role in generating anxiety-related firing patterns. As expected, there was no difference in EPM scores comparing units that followed dHPC to those that did not (Figure 9E).

mPFC single unit activity is correlated with behavioral display of anxiety

mPFC single units appear to differentiate between safe and aversive locations in the EPM. However, it is unclear whether this feature of mPFC activity is related to behavioral measures of anxiety in the EPM. In order to investigate this hypothesis, the mean EPM score for each animal was calculated for all mice with at least three simultaneously recorded single units in the EPM. Mean EPM scores per animal were significantly positively correlated with open arm exploration ($r=+0.65$, Figure 10A). Thus, in animals that display behavioral avoidance of the open arms (dark grey points in Figure 10A), mPFC single units show *less* differentiation between open and closed arms.

To strengthen this association of EPM scores with anxiety-like behavior, we calculated EPM scores in serotonin 1A receptor knockout (5-HT1AR KO) mice. 5-HT1AR KO mice have a robust phenotype of increased anxiety, as well as increased strength of vHPC and mPFC theta oscillations, when exposed to the EPM (Gross et al., 2002; Klemenhagen et al., 2006; Ramboz et al., 1998; Adhikari et al., 2010). In agreement with the unexpected result that lower EPM scores are associated with higher avoidance, 5-HT1AR KO mice had lower EPM scores than WT mice (Figure 10B–C). Indeed, the distributions of EPM scores of avoidant WT mice (those that spent <50% time in the open arms) and 5-HT1AR KO mice were not significantly different from the chance distribution of EPM scores generated after randomly shuffling spike location (Wilcoxon's test, $p<0.79$), suggesting that these mice fail to form appropriate representations of the EPM in the mPFC. This result is consistent with the notion that the failure to represent the EPM is related to anxiety.

Why would mice that avoid the aversive arms fail to develop mPFC representations of aversiveness? One clue comes from overall firing rates. Mean absolute firing rates in the EPM tended to be higher in avoidant WT and 5-HT1AR KO mice compared to WT mice that failed to avoid the open arms (mean+/− s.e.m. firing rate= 2.8 ± 0.58 and 2.94 ± 0.80 Hz for avoidant WT and 5-HT1AR KO mice, respectively, compared to 1.57 ± 0.3 Hz for non-avoidant WT mice). There were no significant differences in the firing rates between these groups in recordings obtained in a control, non-anxiogenic familiar environment. Thus, the elevated firing rates in the EPM of avoidant mice are a consequence of greater increases in rate relative to the familiar environment (Figure 10D). These increases are significant only in avoidant WT and 5-HT1AR KO mice (Wilcoxon's test, $p<0.05$). This result suggests the intriguing possibility that aversion-preferring mPFC units in these animals generalize across open and closed arms of the maze, raising overall firing rates and signaling anxiety regardless of maze location.

DISCUSSION

The vHPC-mPFC circuit has been previously implicated in anxiety by both lesion and neurophysiological data (Adhikari et al., 2010b; Kjelstrup et al., 2002; Shah and Treit, 2004). Based on these findings, we hypothesized that vHPC input might be used by the mPFC to construct a representation of the aversive features of the EPM, which in turn could be used to guide avoidance behavior. Consistent with this hypothesis, we demonstrate here that mPFC units represent safe and aversive arms in the elevated plus maze, regardless of the geometric arrangement of the arms or the stimulus causing aversion. Moreover, firing rates of task-related neurons changed in anticipation of behavior, consistent with a role for

these neurons in guiding exploration in the EPM. Also in line with our predictions, this representation was strongest in those neurons that were significantly modulated by vHPC theta oscillations. These data demonstrate that the mPFC represents the aversive structure of the EPM, and argue that this representation is supported by inputs from the vHPC.

If this representation were indeed used to generate avoidance of the open arms, we would predict that animals with the strongest mPFC representations of the maze would be those that avoided the open arms the most. Surprisingly, however, we found the exact opposite. mPFC single units that represented the aversiveness of the arms were found principally in those animals that *failed* to avoid the open arms. Indeed, in animals that avoided the open arms, units were no more likely to represent these features than would be expected by chance. These results provide a nuanced view of the role of mPFC activity and the vHPC-mPFC circuit in innate anxiety paradigms as discussed below.

An immediate representation of aversiveness in the mPFC

Our data clearly demonstrate that the population of mPFC units differentiates between safe and aversive arms of the EPM. These findings are consistent with the extensive literature demonstrating that task parameters modulate the firing properties of mPFC neurons across a variety of cognitive tasks in highly-trained animals (Burgos-Robles et al., 2009; Fujisawa et al., 2008; Jung et al., 1998; Rich and Shapiro, 2009), which is expected, considering the involvement of the mPFC in diverse cognitive tasks (Birrell and Brown, 2000; Broersen and Uylings, 1999; Farovik et al., 2008; Gemmell et al., 2002; Kesner and Holbrook, 1987; Kolb et al., 1974; Swerdlow et al., 1995; Tait et al., 2009). Our data build on these findings by extending them to an anxiety paradigm in which animals freely explore a novel environment. Using the EPM, we show that mPFC units can display paradigm-related activity in a task that does not involve operant behavior, overt rewards or external reinforcement. The mPFC representation of the task formed immediately – in at least the first 90 seconds, as soon as it could reliably be measured -- without any prior exposure to the task (and thus no learning).

Intriguingly, this representation is linked to input specifically from the vHPC. Numerous reports have demonstrated synchrony between mPFC units and ongoing oscillations in its inputs, particularly the hippocampus (Adhikari et al., 2010a; Jones and Wilson, 2005; Siapas et al., 2005; Sigurdsson et al., 2010a; Taxidis et al., 2010). Here, we show similar synchrony between mPFC units and ongoing theta-frequency oscillations in the ventral, but not dorsal HPC, consistent with the known roles of these subregions in EPM behavior (Kjelstrup et al., 2002). Moreover, we demonstrate that units that synchronize with the vHPC have stronger task-related firing patterns. This effect of synchrony on EPM representations suggests that paradigm-related activity in the mPFC is at least facilitated by input from the vHPC. Consistent with this idea, firing in anticipation of a reward in mPFC units is abolished after vHPC lesions (Burton et al., 2009).

The relationship between mPFC representations and avoidance behavior

Here we demonstrate that mPFC representations and open-arm avoidance are inversely correlated. Animals with mPFC units with strong representations of open vs. closed arms are those that fail to avoid the open arms. At the very least, these data argue that the representation present in the mPFC is not used to guide avoidance behavior in avoidant animals; there is no evidence that such a representation exists in these mice. The role of the mPFC representation in the behavior of animals that fail to avoid the open arms is less clear; the time course of unit firing during arm transitions allows for the possibility that such representations help guide choice behavior during exploration.

A causal relationship between the single unit representation and exploratory behavior is also suggested by the inconsistent effects of mPFC inactivation on EPM behavior in rodents. Some studies report anxiolytic effects (Deacon et al., 2003; Lacroix et al., 2000; Shah et al., 2004; Shah and Treit, 2003, 2004; Stern et al., 2010), while others report anxiogenic or no effects (Klein et al., 2010; Lisboa et al., 2010; Sullivan and Gratton, 2002). Consistent with our findings, studies that reported anxiolytic effects of silencing or lesioning the mPFC were those in which the control group showed relatively low levels of anxiety (Figure S3). mPFC inactivation, therefore, appears to reduce open arm exploration only in those animals that would be expected to have robust mPFC representations.

The role of vHPC inputs to the mPFC in anxiety

Reconciling the current data with our previous findings presents something of a challenge. We have previously shown that increased theta-frequency synchrony between the vHPC and mPFC is associated with increased open arm avoidance (Adhikari et al., 2010). The current data demonstrate that mPFC neurons that represent safety vs. aversiveness are preferentially synchronized to the vHPC. Yet those animals that avoid the open arms – the very animals with the greatest vHPC-mPFC synchrony – do not have the representation that seemingly depends on this synchrony. We propose two possible explanations for this discrepancy.

The first explanation is that avoidant mice generalize – that even though the closed arms are recognized as being slightly safer, the entire maze is seen as threatening. In this scheme, vHPC inputs to the mPFC signal aversiveness throughout the maze, leading to increased vHPC-mPFC synchrony overall, and decreased ability of the mPFC neurons to distinguish between open and closed arms. Our finding of increased absolute firing rates in the high-avoidance WT and 5-HT1AR KO mice are consistent with this conjecture, as are previous results demonstrating increased fear generalization in 5-HT1AR KO mice (Klemenhagen et al., 2006) and reports showing correlations between mPFC activity and fear (Burgos-Robles et al., 2009).

The second explanation posits that the strength of vHPC input to the mPFC is crucial. In this scheme, under conditions of low anxiety, moderately active vHPC inputs signaling aversiveness are integrated with other inputs (carrying, for example, spatial information) and utilized by the mPFC to construct a paradigm-specific map of the EPM. Under conditions of high anxiety, vHPC inputs are too strong, swamping out other inputs and leading to a failure of the mPFC to construct this map. This latter explanation posits the mPFC representation as a cognitive mechanism, capable of guiding exploratory behavior only under conditions where the emotional imperative – avoidance – fails to trump cognition.

In either scheme, under conditions of low anxiety, mPFC activity makes use of threat information to guide careful exploration of the maze. The anxiolytic effects of mPFC lesions occur because, in the absence of a functional mPFC, exploratory drive wins out without consideration of this threat information. Under conditions of high anxiety, however, the principal driver of avoidance behavior moves elsewhere, and the mPFC is no longer necessary to drive threat avoidance. While alternative interpretations are possible, the notion that activity in the mPFC has a uniform relationship with innate anxiety behaviors is certainly challenged by the current dataset.

Conclusion

Our data demonstrate that the mPFC is capable of generating a representation of an anxiogenic environment. The findings further suggest that it does so with the help of input from the vHPC, providing an important link between two well-documented aspects of mPFC unit activity: task-related firing patterns and synchrony with hippocampal input. When

considered in the context of lesion data, our data suggest that under the right conditions the mPFC may use its representation of the EPM to guide exploratory behavior. A complete explanation of the neural activity underlying innate anxiety-like behavior will require additional studies aimed at a broader array of structures.

EXPERIMENTAL PROCEDURES

Animals

Three to six month old male 129Sv/Ev mice were obtained from Taconic (Germantown, NY, USA). Twenty-seven wild type and four 5-HT1AR knockout mice were used. 5-HT1AR knockout mice were generated from heterozygote breeding pairs on a 129SvEvTac background as described previously (Ramboz et al., 1998). The procedures described here were conducted in accordance with National Institutes of Health regulations and approved by the Columbia University and New York State Psychiatric Institute Institutional Animal Care and Use Committees.

Microdrive Construction

Microdrives were built as described previously (Adhikari et al., 2010b). Briefly, Custom microdrives were constructed using interface boards (EIB-16, Neuralynx, Bozeman, MT) fastened to machine screws (SHCX-080-6, Small Parts, Inc, Miramar, FL). Stereotrodes (4–6 per animal) were constructed of 25 μM Formvar-coated tungsten micro wire (California Fine Wire, Grover Beach, CA), fastened to a cannula attached to the interface board, and implanted in the mPFC. Single wire, 75 μM tungsten electrodes were stereotactically placed into the HPC and cemented directly to the skull during surgery.

Surgery

Surgical procedures have been described elsewhere (Adhikari et al., 2010b). Briefly, animals were anesthetized with ketamine and xylazine (165 and 5.5 mg/kg, in saline) supplemented with inhaled isoflurane (0.5–1%) in oxygen, and placed in a stereotactic apparatus (Kopf Instruments, Tujunga, CA) on a feedback-controlled heating pad. Anterior-posterior and medial-lateral coordinates were measured from bregma, while depth was calculated relative to brain surface. Tungsten wire electrodes were implanted in the dHPC CA1 (−1.94 mm AP, 1.5 mm LM and 1.4 mm DV), vHPC CA1 (−3.16, 3.0 and 4.2) and mPFC (+1.65, 0.5, and 1.5), resulting in tip locations near the fissure or in the stratum lacunosum-moleculare for the HPC electrodes, and in the deep layers of the prelimbic cortex for mPFC electrodes (Figure S4). Animals were given analgesics (Carprofen, 5 mg/kg S.C.) and monitored postoperatively.

Behavioral Protocol

Animals were permitted to recover for at least one week or until regaining pre-surgery body weight, and then food restricted to 85% body weight. During food restriction animals were familiarized to the recording setup and handling by being tethered to the head stage in their home cages for 5–7 daily sessions of 20 minutes each. Mice were exposed to either to the standard or to one of the altered versions of the EPM for 10 minutes. A resting period of one hour separated the two EPM exposures in experiments in which recordings from the same single unit were obtained in two different EPM configurations.

The EPM was chosen for this work because it is a standard anxiety paradigm with pharmacological validity (Cruz et al., 1994; Pellow and File, 1986). The EPM also has well-defined boundaries between the more aversive (open arms) and the safe areas (closed arms). Exposures to the standard EPM were done at 200 lux. The EPM was constructed of wood painted grey and consisted of four arms, 7.6 cm wide and 28 cm long, elevated 31 cm above

the floor. 15-cm-high walls enclosed two opposing arms, whereas two arms were open, except for a 1-cm-high lip at the edge. Time spent in open arms was highly correlated across multiple exposures to the EPM in a subset of the animals exposed to the EPM twice ($r=0.8$, $p<0.01$), Furthermore, in a subset of mice exposed to both the EPM and the open field (an anxiety paradigm in which the center is the aversive area), time spent in the open arms of the EPM and center of the open field were highly correlated ($r=0.45$, $p<0.05$). These data suggest that behavioral measures used in the current work reflect trait-anxiety.

Altered EPMs were used for the analyses in Figures 5 and 6. All mazes had identical dimensions to the standard maze. For Figure 5, the arrangement of the arms was altered, such that open arms are adjacent to each other (Figure 5A). For Figure 6, mice were exposed to the standard EPM in the dark, and to an EPM with four closed arms, two of them brightly lit (600 lux). The order of presentation of the mazes was counterbalanced across animals. Animals avoide the aversive arms in each maze equally (Figure 7I). Furthermore, mPFC theta power was higher in the safe arms of all the EPM configurations used (Figure S5), in agreement with previous reports of mPFC theta power being higher in the safe closed arms of the EPM compared to the open arms (Adhikari et al., 2010b).

Data Acquisition

mPFC stereotrodes were advanced until at least four well-isolated single units could be recorded. Recordings were obtained via a unitary gain head-stage preamplifier (HS-16; Neuralynx) attached to a fine wire cable. Field potential signals from HPC and mPFC sites were recorded against a screw implanted in the anterior portion of the skull. LFPs were amplified, bandpass filtered (1–1000 Hz) and acquired at 1893 Hz. Spikes exceeding 40 μV were bandpass-filtered (600–6000 Hz) and recorded at 32 kHz. Both LFP and spike data were acquired with Lynx 8 programmable amplifiers on a personal computer running Cheetah data acquisition software (Neuralynx). The animal's position was obtained by overhead video tracking (30 Hz) of two light-emitting diodes affixed to the head stage.

Data Analysis

Data was imported into Matlab for analysis using custom-written software. Velocity was calculated from position records and smoothed using a window of 0.33 seconds. Clustering of spikes was performed offline manually with SpikeSort 3D (Neuralynx). Cluster isolation quality was assessed by calculating L ratio and isolation distance measurements for all clusters (Schmitzer-Torbert et al., 2005). Cluster isolation quality measures (Figure S6, mean and median L ratio = 0.13 ± 0.03 and 0.021, and mean and median isolation distance = 61.2 ± 10.2 and 35, respectively) were similar to those of previously published reports (Schmitzer-Torbert et al., 2005). Cluster isolation quality was not correlated with EPM scores (Figure S6), indicating that cells with low EPM scores are not poorly isolated. Mean firing rates (2.05 ± 0.64) and waveform features were similar to previous reports (Bartho et al., 2004), and suggest that the majority of the units are putative pyramidal cells. None of the results shown were correlated with firing rates, waveform features or cortical layer.

Only cells with more than 100 spikes were used in all analyses, unless otherwise stated. Out of 79 units, 69 had more than 100 spikes in the 10-minute EPM exploration session. Results were not affected by the choice of a minimum number of spikes, provided this number was above 50.. Only data from mice that explored all arms of the maze were used. In total, 191 units with more than 100 spikes were recorded from 27 mice. 69 units were recorded in the standard EPM (18 of these units were also recorded in the altered modular EPM), 122 units in the EPM in the dark (of which 105 were recorded also in the EPM with four closed arms). Mean firing rates did not differ across environments.

To identify the fraction of units significantly modulated by arm type an ANOVA was computed on the firing rate of each unit using arm type as a factor with three levels (center, closed arms and open arms). EPM scores were computed to quantify the degree to which the firing pattern of a single unit is anxiety-related. EPM scores were calculated through the following formula:

$$\text{Score}=(A - B)/(A+B),$$

where

$A=0.25*(|F_L-F_U|+|F_L-F_D|+|F_R-F_U|+|F_R-F_D|)$ and

$B=0.5*(|F_L-F_R|+|F_U-F_D|)$.

F_L, F_R, F_U and F_D are the % difference from mean firing rate in left, right, up and down arms, respectively. A is the mean difference in normalized firing rate between arms of different types, while B is the mean difference for arms of the same type. Cells with firing patterns related to the task have similar firing rates in arms of the same type (resulting in a small B) and large differences in rates between arms of different types (resulting in a large value for A). The maximum score of 1.0 indicates no difference in firing rates across arms of the same type (B=0). Negative scores indicate that firing rates are more similar across arms of different types than across arms of the same type.

The significance of the distribution of EPM scores was calculated using bootstrapping. For each unit with n spikes, a simulated distribution of scores was generated by calculating the EPM score of n randomly chosen timestamps 500 times. This generated a distribution with 500*69 scores, where 69 is the number of units recorded in the standard EPM at 200 Lux. The significance of the experimentally observed EPM score was calculated by comparing it to the simulated distribution using Wilcoxon's test.

In order to study the activity of mPFC units at transitions between compartments, firing rate z-scores were calculated for each unit for 10-second periods centered around each transition points, averaged across all transitions for each cell. These firing rate timecourses were then averaged across all units of the same type. Change point analysis (Gallistel et al., 2004) was used to identify the sample at which unit activity started to change. Briefly, this method identifies a point in which there is a change in the slope of the cumulative sum of the time series of interest, which in this case is the averaged single unit firing z-scores. The data is then divided in two parts: the first is comprised of all the data preceding the change point and the second is the data occurring after the putative change point. The non-parametric Kolmogorov-Smirnov test is then used to assess if these two segments of data have significantly different means ($p<0.01$). If the two means differ significantly, then the identified point is considered a sample at which a significant change in the time series being measured has occurred. After one change point is identified, the data is truncated, such that all the data preceding the change point is ignored. The algorithm described above is then repeated, so that a new change point, if any, can be found. This analysis only identified one significant change point per plot. For the change point analysis, 0.25 sec bins were used to allow for higher temporal resolution, and the data were not smoothed. To provide better visualization of the data, larger, 0.5 sec smoothed bins were used for the graphs in Figure 5. As shown in Figure 5, firing rates differ before and after the animal leaves or enters the closed arms. This is in line with the finding that firing rates in the closed arms are negatively correlated to both firing in the center ($r= -0.54$, $p<0.0001$) and in the open arms ($r= -0.64$, $p<0.0001$). Change points were estimated using the MATLAB function cp_wrapper, available online (Gallistel et al., 2004), with the inputs change_points=cp_wrapper(averaged_z scores, 0,2,2), which results in the selection of a

Kolmogorov-Smirnov test and logit=2, where logit=log10((1-p_value)/p_value), resulting in a p_value of 0.01. Population principal components during EPM transitions were calculated with the MATLAB function princomp. mPFC units recorded in the standard EPM at 200 lux and in the standard EPM at zero lux were pooled for this analysis.

Phase locking analysis was conducted as described (Sigurdsson et al., 2010b). Briefly, each spike was assigned a theta phase derived from a Hilbert transform of the simultaneously recorded, theta-frequency filtered LFP. The mean resultant length vector (MRL) value was computed as a measure of phase-locking strength, and significance was determined by Rayleigh's test for circular uniformity. To determine directionality, MRL was calculated for 40 different temporal offsets for each single unit spike train; directionality was determined by the location of the peak MRL value for cells with significant phase-locking after correction for multiple comparisons.

Histology and Genotype Confirmation

Upon the completion of recording, animals were deeply anesthetized; electrolytic lesions were made to verify electrode positions; and animals were then perfused with formalin. Brain sections were mounted on slides to visualize and photograph lesions. For 5-HT1AR knockouts and control littermates, tail DNA was extracted to reconfirm genotype through PCR.

Statistics

Paired Wilcoxon's signed rank non-parametric tests were used throughout, unless otherwise stated. All statistically significant correlations were significant with both Spearman's and Pearson's methods; Spearman's correlations are reported as they are less sensitive to outliers and requires a monotonic, but not necessarily linear, relationship. All correlation values on figures are plotted with a 95% confidence interval and p value obtained from bootstrapping. Standard errors of means (S.E.Ms) were plotted in bar graphs to show the accuracy of the estimation of the mean of the population.

Supplementary Material

Refer to Web version on PubMed Central for supplementary material.

Acknowledgments

We thank E. B. Likhtik, P.T. O'Neill, R. Hen and T. Sigurdsson for comments on the manuscript, as well as H. Moore and the members of the Gordon and Hen labs for helpful discussions of the experimental design and analysis. This work was supported by grants to J.A.G. from the NIMH (K08 MH098623 and R01 MH081958) and the Hope for Depression Research Foundation. J.A.G. is also the recipient of the IMHRO Rising Star Award.

References

Adhikari A, Sigurdsson T, Topiwala MA, Gordon JA. Cross-correlation of instantaneous amplitudes of field potential oscillations: a straightforward method to estimate the directionality and lag between brain areas. J Neurosci Methods. 2010a; 191:191–200. [PubMed: 20600317]

Adhikari A, Topiwala MA, Gordon JA. Synchronized activity between the ventral hippocampus and the medial prefrontal cortex during anxiety. Neuron. 2010b; 65:257–269. [PubMed: 20152131]

Bannerman DM, Deacon RM, Offen S, Friswell J, Grubb M, Rawlins JN. Double dissociation of function within the hippocampus: spatial memory and hyponeophagia. Behav Neurosci. 2002; 116:884–901. [PubMed: 12369808]

Bannerman DM, Rawlins JN, McHugh SB, Deacon RM, Yee BK, Bast T, Zhang WN, Pothuizen HH, Feldon J. Regional dissociations within the hippocampus--memory and anxiety. Neurosci Biobehav Rev. 2004; 28:273–283. [PubMed: 15225971]

Bartho P, Hirase H, Monconduit L, Zugaro M, Harris KD, Buzsaki G. Characterization of neocortical principal cells and interneurons by network interactions and extracellular features. J Neurophysiol. 2004; 92:600–608. [PubMed: 15056678]

Birrell JM, Brown VJ. Medial frontal cortex mediates perceptual attentional set shifting in the rat. J Neurosci. 2000; 20:4320–4324. [PubMed: 10818167]

Broersen LM, Uylings HB. Visual attention task performance in Wistar and Lister hooded rats: response inhibition deficits after medial prefrontal cortex lesions. Neuroscience. 1999; 94:47–57. [PubMed: 10613496]

Burgos-Robles A, Vidal-Gonzalez I, Quirk GJ. Sustained conditioned responses in prelimbic prefrontal neurons are correlated with fear expression and extinction failure. J Neurosci. 2009; 29:8474–8482. [PubMed: 19571138]

Burgos-Robles A, Vidal-Gonzalez I, Santini E, Quirk GJ. Consolidation of fear extinction requires NMDA receptor-dependent bursting in the ventromedial prefrontal cortex. Neuron. 2007; 53:871–880. [PubMed: 17359921]

Burton BG, Hok V, Save E, Poucet B. Lesion of the ventral and intermediate hippocampus abolishes anticipatory activity in the medial prefrontal cortex of the rat. Behav Brain Res. 2009; 199:222–234. [PubMed: 19103227]

Cacucci F, Wills TJ, Lever C, Giese KP, O'Keefe J. Experience-dependent increase in CA1 place cell spatial information, but not spatial reproducibility, is dependent on the autophosphorylation of the alpha-isoform of the calcium/calmodulin-dependent protein kinase II. J Neurosci. 2007; 27:7854–7859. [PubMed: 17634379]

Calza A, Sogliano C, Santoru F, Marra C, Angioni MM, Mostallino MC, Biggio G, Concas A. Neonatal exposure to estradiol in rats influences neuroactive steroid concentrations, GABAA receptor expression, and behavioral sensitivity to anxiolytic drugs. J Neurochem. 2010; 113:1285–1295. [PubMed: 20345753]

Chapin JK. Using multi-neuron population recordings for neural prosthetics. Nat Neurosci. 2004; 7:452–455. [PubMed: 15114357]

Cruz AP, Frei F, Graeff FG. Ethopharmacological analysis of rat behavior on the elevated plus-maze. Pharmacol Biochem Behav. 1994; 49:171–176. [PubMed: 7816869]

Deacon RM, Penny C, Rawlins JN. Effects of medial prefrontal cortex cytotoxic lesions in mice. Behav Brain Res. 2003; 139:139–155. [PubMed: 12642185]

Farovik A, Dupont LM, Arce M, Eichenbaum H. Medial prefrontal cortex supports recollection, but not familiarity, in the rat. J Neurosci. 2008; 28:13428–13434. [PubMed: 19074016]

Favaro PN, Costa LC, Moreira EG. Maternal fluoxetine treatment decreases behavioral response to dopaminergic drugs in female pups. Neurotoxicol Teratol. 2008; 30:487–494. [PubMed: 18586456]

Frassetto SS, Alves IO, Santos MM, Schmidt AE, Lopes JJ, Oliveira PA, Vinagre AS, Pereira P. Absence of sibutramine effect on spontaneous anxiety in rats. Arq Bras Endocrinol Metabol. 2010; 54:375–380. [PubMed: 20625649]

Fujisawa S, Amarasingham A, Harrison MT, Buzsaki G. Behavior-dependent short-term assembly dynamics in the medial prefrontal cortex. Nat Neurosci. 2008; 11:823–833. [PubMed: 18516033]

Gallistel CR, Fairhurst S, Balsam P. The learning curve: implications of a quantitative analysis. Proc Natl Acad Sci U S A. 2004; 101:13124–13131. [PubMed: 15331782]

Gemmell C, Anderson M, O'Mara SM. Deep layer prefrontal cortex unit discharge in a cue-controlled open-field environment in the freely-moving rat. Behav Brain Res. 2002; 133:1–10. [PubMed: 12048169]

Gomes PB, Feitosa ML, Silva MI, Noronha EC, Moura BA, Venancio ET, Rios ER, de Sousa DP, de Vasconcelos SM, Fonteles MM, de Sousa FC. Anxiolytic-like effect of the monoterpene 1,4-cineole in mice. Pharmacol Biochem Behav. 2010; 96:287–293. [PubMed: 20670917]

Gonzalez LE, Rujano M, Tucci S, Paredes D, Silva E, Alba G, Hernandez L. Medial prefrontal transection enhances social interaction. I: behavioral studies. Brain Res. 2000; 887:7–15. [PubMed: 11134584]

Gross C, Zhuang X, Stark K, Ramboz S, Oosting R, Kirby L, Santarelli L, Beck S, Hen R. Serotonin1A receptor acts during development to establish normal anxiety-like behaviour in the adult. Nature. 2002; 416:396–400. [PubMed: 11919622]

Guilloux JP, David DJ, Xia L, Nguyen HT, Rainer Q, Guiard BP, Reperant C, Delthei T, Toth M, Hen R, Gardier AM. Characterization Of 5-HT1A/1B−/− Mice: An Animal Model Sensitive To Anxiolytic Treatments. Neuropharmacology. 2011

Hogg S. A review of the validity and variability of the elevated plus-maze as an animal model of anxiety. Pharmacol Biochem Behav. 1996; 54:21–30. [PubMed: 8728535]

Jones MW, Wilson MA. Theta rhythms coordinate hippocampal-prefrontal interactions in a spatial memory task. PLoS Biol. 2005; 3:e402. [PubMed: 16279838]

Jung MW, Qin Y, McNaughton BL, Barnes CA. Firing characteristics of deep layer neurons in prefrontal cortex in rats performing spatial working memory tasks. Cereb Cortex. 1998; 8:437–450. [PubMed: 9722087]

Kanegawa N, Suzuki C, Ohinata K. Dipeptide Tyr-Leu (YL) exhibits anxiolytic-like activity after oral administration via activating serotonin 5-HT1A, dopamine D1 and GABAA receptors in mice. FEBS Lett. 2009; 584:599–604. [PubMed: 20005875]

Kesner RP, Holbrook T. Dissociation of item and order spatial memory in rats following medial prefrontal cortex lesions. Neuropsychologia. 1987; 25:653–664. [PubMed: 3658148]

Kjelstrup KG, Tuvnes FA, Steffenach HA, Murison R, Moser EI, Moser MB. Reduced fear expression after lesions of the ventral hippocampus. Proc Natl Acad Sci U S A. 2002; 99:10825–10830. [PubMed: 12149439]

Klein J, Winter C, Coquery N, Heinz A, Morgenstern R, Kupsch A, Juckel G. Lesion of the medial prefrontal cortex and the subthalamic nucleus selectively affect depression-like behavior in rats. Behav Brain Res. 2010; 213:73–81. [PubMed: 20434489]

Klemenhagen KC, Gordon JA, David DJ, Hen R, Gross CT. Increased fear response to contextual cues in mice lacking the 5-HT1A receptor. Neuropsychopharmacology. 2006; 31:101–111. [PubMed: 15920501]

Kolb B, Nonneman AJ, Singh RK. Double dissociation of spatial impairments and perseveration following selective prefrontal lesions in rats. J Comp Physiol Psychol. 1974; 87:772–780. [PubMed: 4426996]

Kumar R, Murugananthan G, Nandakumar K, Talwar S. Isolation of anxiolytic principle from ethanolic root extract of Cardiospermum halicacabum. Phytomedicine. 2011; 18:219–223. [PubMed: 20732800]

Lacroix L, Spinelli S, Heidbreder CA, Feldon J. Differential role of the medial and lateral prefrontal cortices in fear and anxiety. Behav Neurosci. 2000; 114:1119–1130. [PubMed: 11142644]

Leggio GM, Micale V, Le Foll B, Mazzola C, Nobrega JN, Drago F. Dopamine D(3) receptor knock-out mice exhibit increased behavioral sensitivity to the anxiolytic drug diazepam. Eur Neuropsychopharmacol. 2010

Lisboa SF, Stecchini MF, Correa FM, Guimaraes FS, Resstel LB. Different role of the ventral medial prefrontal cortex on modulation of innate and associative learned fear. Neuroscience. 2010; 171:760–768. [PubMed: 20883749]

Melo FH, Venancio ET, de Sousa DP, de Franca Fonteles MM, de Vasconcelos SM, Viana GS, de Sousa FC. Anxiolytic-like effect of Carvacrol (5-isopropyl-2-methylphenol) in mice: involvement with GABAergic transmission. Fundam Clin Pharmacol. 2009; 24:437–443. [PubMed: 19909350]

Micale V, Cristino L, Tamburella A, Petrosino S, Leggio GM, Drago F, Di Marzo V. Altered responses of dopamine D3 receptor null mice to excitotoxic or anxiogenic stimuli: Possible involvement of the endocannabinoid and endovanilloid systems. Neurobiol Dis. 2009; 36:70–80. [PubMed: 19591935]

Murphy K, Kubin ZJ, Shepherd JN, Ettinger RH. Valeriana officinalis root extracts have potent anxiolytic effects in laboratory rats. Phytomedicine. 2009; 17:674–678. [PubMed: 20042323]

Nishino T, Takeuchi T, Takechi K, Kamei C. Evaluation of anxiolytic-like effects of some short-acting benzodiazepine hypnotics in mice. J Pharmacol Sci. 2008; 107:349–354. [PubMed: 18603828]

Parent MA, Wang L, Su J, Netoff T, Yuan LL. Identification of the Hippocampal Input to Medial Prefrontal Cortex In Vitro. Cereb Cortex. 2009

Paterson NE, Iwunze M, Davis SF, Malekiani SA, Hanania T. Comparison of the predictive validity of the mirror chamber and elevated plus maze tests in mice. J Neurosci Methods. 2010; 188:62–70. [PubMed: 20149823]

Pellow S, File SE. Anxiolytic and anxiogenic drug effects on exploratory activity in an elevated plus-maze: a novel test of anxiety in the rat. Pharmacol Biochem Behav. 1986; 24:525–529. [PubMed: 2871560]

Peters YM, O'Donnell P, Carelli RM. Prefrontal cortical cell firing during maintenance, extinction, and reinstatement of goal-directed behavior for natural reward. Synapse. 2005; 56:74–83. [PubMed: 15729742]

Pratt WE, Mizumori SJ. Neurons in rat medial prefrontal cortex show anticipatory rate changes to predictable differential rewards in a spatial memory task. Behav Brain Res. 2001; 123:165–183. [PubMed: 11399329]

Ramboz S, Oosting R, Amara DA, Kung HF, Blier P, Mendelsohn M, Mann JJ, Brunner D, Hen R. Serotonin receptor 1A knockout: an animal model of anxiety-related disorder. Proc Natl Acad Sci U S A. 1998; 95:14476–14481. [PubMed: 9826725]

Rich EL, Shapiro M. Rat prefrontal cortical neurons selectively code strategy switches. J Neurosci. 2009; 29:7208–7219. [PubMed: 19494143]

Saiyudthong S, Marsden CA. Acute effects of bergamot oil on anxiety-related behaviour and corticosterone level in rats. Phytother Res. 2010

Schmitzer-Torbert N, Jackson J, Henze D, Harris K, Redish AD. Quantitative measures of cluster quality for use in extracellular recordings. Neuroscience. 2005; 131:1–11. [PubMed: 15680687]

Shah AA, Sjovold T, Treit D. Inactivation of the medial prefrontal cortex with the GABAA receptor agonist muscimol increases open-arm activity in the elevated plus-maze and attenuates shock-probe burying in rats. Brain Res. 2004; 1028:112–115. [PubMed: 15518648]

Shah AA, Treit D. Excitotoxic lesions of the medial prefrontal cortex attenuate fear responses in the elevated-plus maze, social interaction and shock probe burying tests. Brain Res. 2003; 969:183–194. [PubMed: 12676379]

Shah AA, Treit D. Infusions of midazolam into the medial prefrontal cortex produce anxiolytic effects in the elevated plus-maze and shock-probe burying tests. Brain Res. 2004; 996:31–40. [PubMed: 14670628]

Siapas AG, Lubenov EV, Wilson MA. Prefrontal phase locking to hippocampal theta oscillations. Neuron. 2005; 46:141–151. [PubMed: 15820700]

Sigurdsson T, Stark KL, Karayiorgou M, Gogos JA, Gordon JA. Impaired hippocampal–prefrontal synchrony in a genetic mouse model of schizophrenia. Nature. 2010a; 464:763–767. [PubMed: 20360742]

Sigurdsson T, Stark KL, Karayiorgou M, Gogos JA, Gordon JA. Impaired hippocampal prefrontal synchrony in a genetic mouse model of schizophrenia. Nature. 2010b; 464:763–767. [PubMed: 20360742]

Stern CA, Do Monte FH, Gazarini L, Carobrez AP, Bertoglio LJ. Activity in prelimbic cortex is required for adjusting the anxiety response level during the elevated plus-maze retest. Neuroscience. 2010; 170:214–222. [PubMed: 20620194]

Sullivan RM, Gratton A. Behavioral effects of excitotoxic lesions of ventral medial prefrontal cortex in the rat are hemisphere-dependent. Brain Res. 2002; 927:69–79. [PubMed: 11814433]

Swerdlow NR, Lipska BK, Weinberger DR, Braff DL, Jaskiw GE, Geyer MA. Increased sensitivity to the sensorimotor gating-disruptive effects of apomorphine after lesions of medial prefrontal cortex or ventral hippocampus in adult rats. Psychopharmacology (Berl). 1995; 122:27–34. [PubMed: 8711061]

Tait DS, Marston HM, Shahid M, Brown VJ. Asenapine restores cognitive flexibility in rats with medial prefrontal cortex lesions. Psychopharmacology (Berl). 2009; 202:295–306. [PubMed: 18925388]

Taxidis J, Coomber B, Mason R, Owen M. Assessing cortico-hippocampal functional connectivity under anesthesia and kainic acid using generalized partial directed coherence. Biol Cybern. 2010; 102:327–340. [PubMed: 20204395]

Umathe SN, Bhutada PS, Jain NS, Dixit PV, Wanjari MM. Effects of central administration of gonadotropin-releasing hormone agonists and antagonist on elevated plus-maze and social interaction behavior in rats. Behav Pharmacol. 2008; 19:308–316. [PubMed: 18622178]

Venancio ET, Rocha NF, Rios ER, Feitosa ML, Linhares MI, Melo FH, Matias MS, Fonseca FN, Sousa FC, Leal LK, Fonteles MM. Anxiolytic-like effects of standardized extract of Justicia pectoralis (SEJP) in mice: Involvement of GABA/benzodiazepine in receptor. Phytother Res. 2010

Verwer RW, Meijer RJ, Van Uum HF, Witter MP. Collateral projections from the rat hippocampal formation to the lateral and medial prefrontal cortex. Hippocampus. 1997; 7:397–402. [PubMed: 9287079]

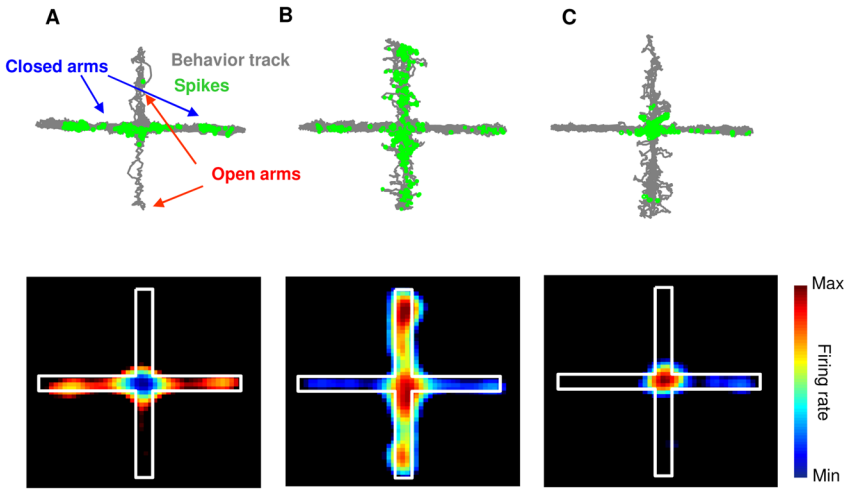

Figure 1. mPFC single units have task-related firing patterns in the EPM

(A-C) Upper panels: Spatial distributions of spikes of representative single units that fired preferentially in the closed (A) or open (B) arms or the center (C) of the EPM. The behavior track is shown in grey and the location of occurrence of each spike is marked with a green circle. Lower Panel: Spatial firing rate maps of the same single units. Average normalized firing rates are color-coded (higher firing rates are indicated by warmer colors) for each pixel. See also Figure S4.

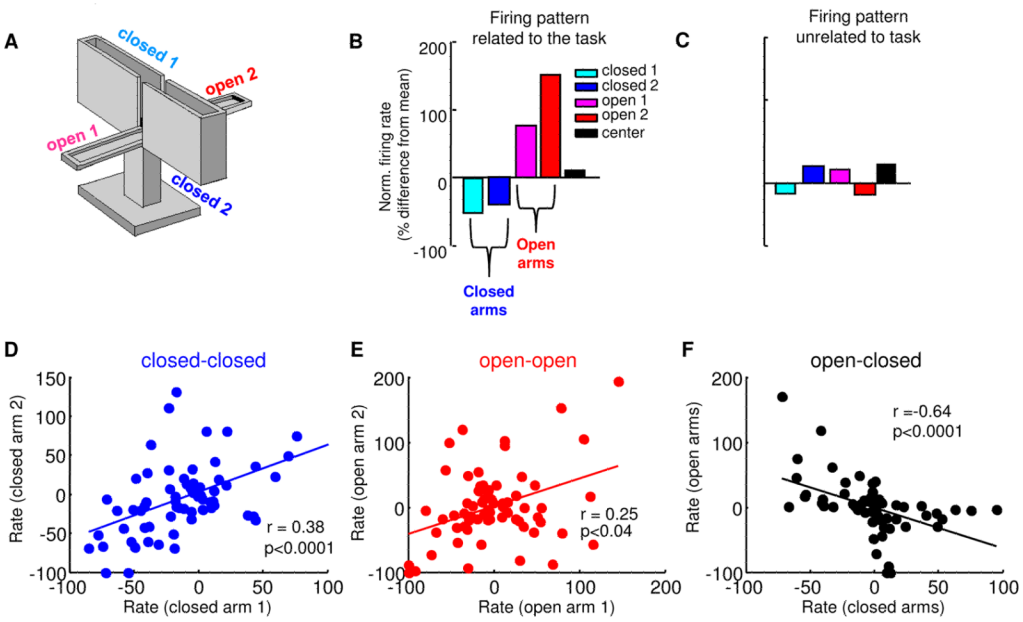

Figure 2. mPFC single units differentiate between open and closed arms in the EPM

(A) Depiction of the standard EPM. (B,C) Normalized firing rates (% difference from mean firing rate) from each of the arms for representative units with putative task-related (B) and task-unrelated (C) firing patterns. (D) Scatter plot of normalized firing rates (% difference form mean rate) across both closed arms for all recorded units with > 100 total spikes. Each point represents a single unit. Note that normalized rates in the closed arms are strongly positively correlated (r=0.38, p<0.0001, n=69 cells). (E) Same as (D), but for rates in the two open arms (r= 0.25, p<0.04, n=69 cells). (F) Correlation of normalized rates across closed and open arms. Note that firing rates are negatively correlated across arms of different type (r= −0.64, p<0.0001, n=69 cells). See also Figure S1.

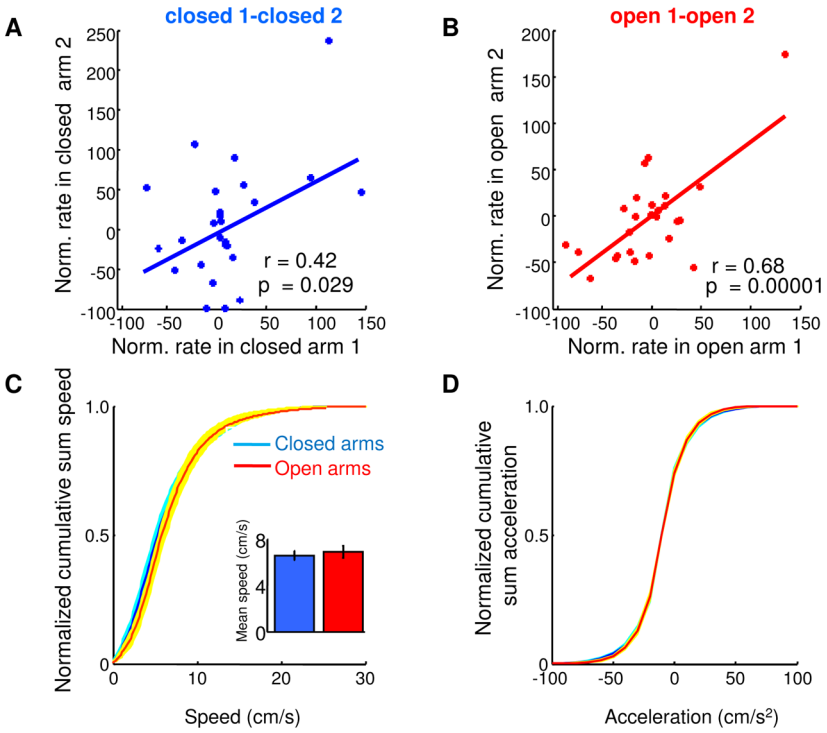

Figure 3. mPFC firing patterns in the EPM are not due to novelty or locomotor differences

(A) Scatter plot of normalized firing rates for mPFC single units in both closed arms during a second ten-minute exposure to the EPM, a day after the original exposure. (B) Same as left panel, but for firing in both open arms. (C) Cumulative sum distribution of speed in the closed and open arms. Inset: Mean +/− s.e.m. speed across animals in the closed and open arms (p=0.56). (D) Cumulative sum distribution of acceleration. Shaded areas are ± s.e.m.

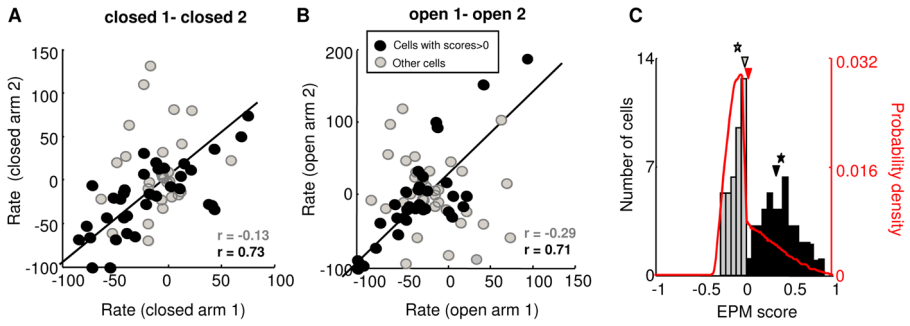

Figure 4. mPFC units with anxiety-related firing patterns are over-represented in the population

(A,B) Cells with positive EPM scores (black circles) have more marked task-related firing than those with negative EPM scores (grey circles), as measured by higher correlations between firing in the two closed (A) and two open (B) arms. Correlation values for grey and black circles are plotted in their respective colors. (C) Distribution of EPM scores for all recorded units with > 100 total spikes. The arrowheads and stars marks the median and mean of the subsamples of units with negative (grey) and positive (black) scores. The distribution differs significantly from that expected by chance (red line). See also Figure S6.

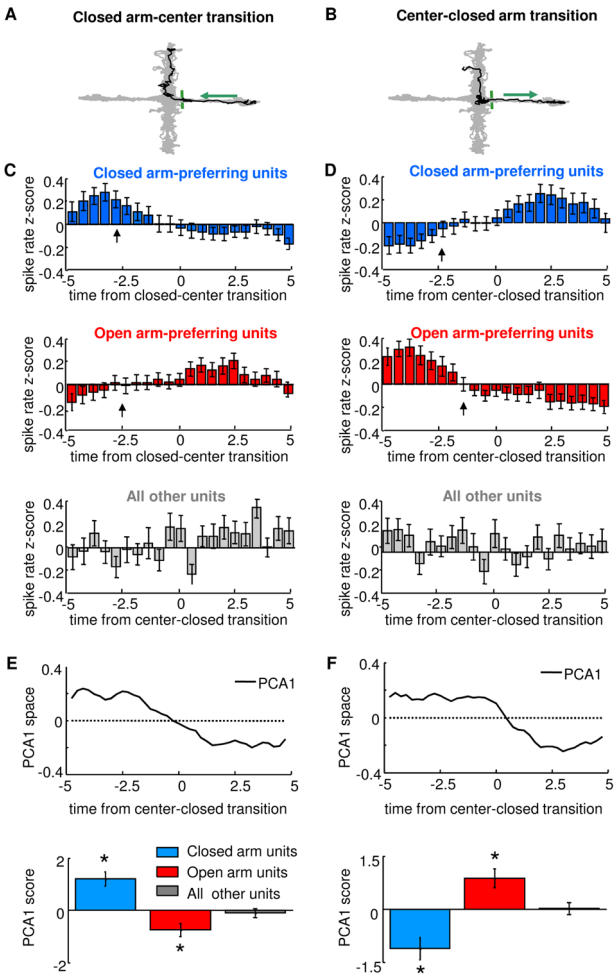

Figure 5. Changes in unit activity precede transitions across compartments in the EPM

(A,B) Representative transitions (black) from the closed arm to the open arm (A) and from the open arm to the closed arm (B), superimposed on the behavioral trace from the entire session (grey). Arrows indicate the direction of movement and the green bars indicates the boundary between closed arm and center. (C,D) Peri-event time histograms averaged across all closed-to-center transitions (C) and center-to-closed transitions (D) for all closed arm-preferring units (blue), open arm-preferring units (red), and for units without task-related firing, as defined by negative EPM scores (grey). Firing rates were converted to Z-scores in 0.5 s bins. Arrows indicate the time point at which significant changes in firing rate begin to occur, as calculated by the change point method ($p<0.01$, see Experimental Procedures). Note that all significant changes in mPFC unit activity occur 1–3 s prior to the animal leaving (C) or entering (D) the closed arm. No significant change points were identified for the units with negative EPM scores. Units recorded in the standard EPM at 200 and 0–5 Lux were pooled for this analysis (n=69 units from the standard EPM at 200 Lux and n=122 units from the standard EPM in the dark). (E) Principal components analysis of firing rates during transitions. Upper panel: first principal component of the entire population of units is shown for closed to center transitions. Note that the curve in has a time-course similar to the firing patterns of closed arm units (C, blue bars). Lower panel: Mean scores of the first principal component (PC1) of closed arm-preferring units, open arm-preferring units and units with negative EPM scores. (F) Same as (E), but for center to closed arm transitions

(n=69 units from the standard EPM at 200 Lux and n=122 units from the standard EPM in the dark, pooled). *p<0.01, Wilcoxon rank sum test. Error bars are ± S.E.M.s.

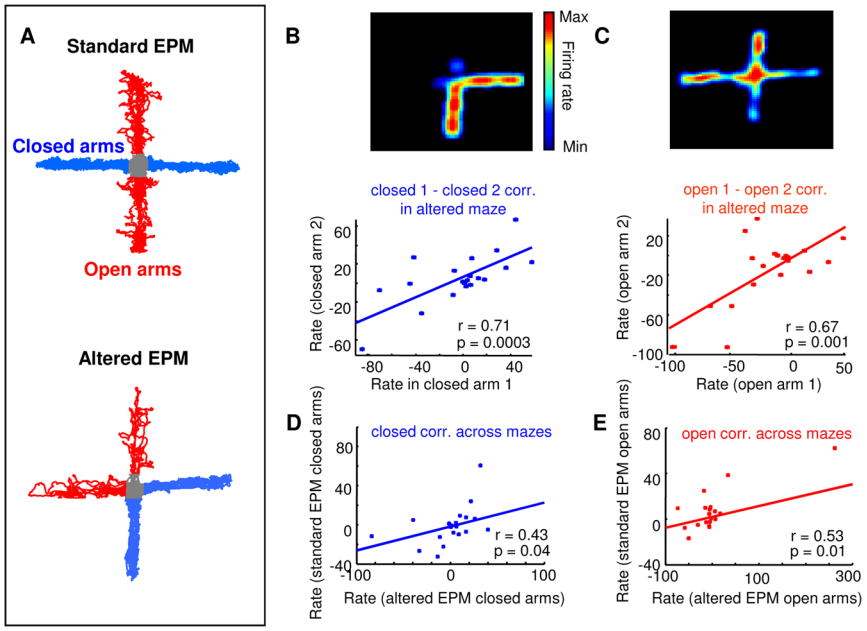

Figure 6. Paradigm-related firing patterns do not depend on the geometric arrangement of the arms

(A) 18 units were recorded during exposure to both the standard EPM (upper panel) and an altered EPM (lower panel) in which arms of the same type were adjacent to each other rather than across from each other. (B, C) Upper panels: Firing rate maps (warmer colors represent higher firing rates) for a units that fired preferentially in the closed (A) and open (C) arms of the altered EPM. Lower panel: Scatter plots of normalized rates (% difference from mean firing rate) for all 18 units across the two closed (B) and open (C) arms in the altered EPM. (D,E) Correlation between firing rates in closed arms (D) and open arms (E) across the two mazes. Firing rates were significantly positively correlated across arms of the same type even across mazes. The correlation in (E) is significant even if the point on the upper right corner is excluded (r=0.46, p=0.04).

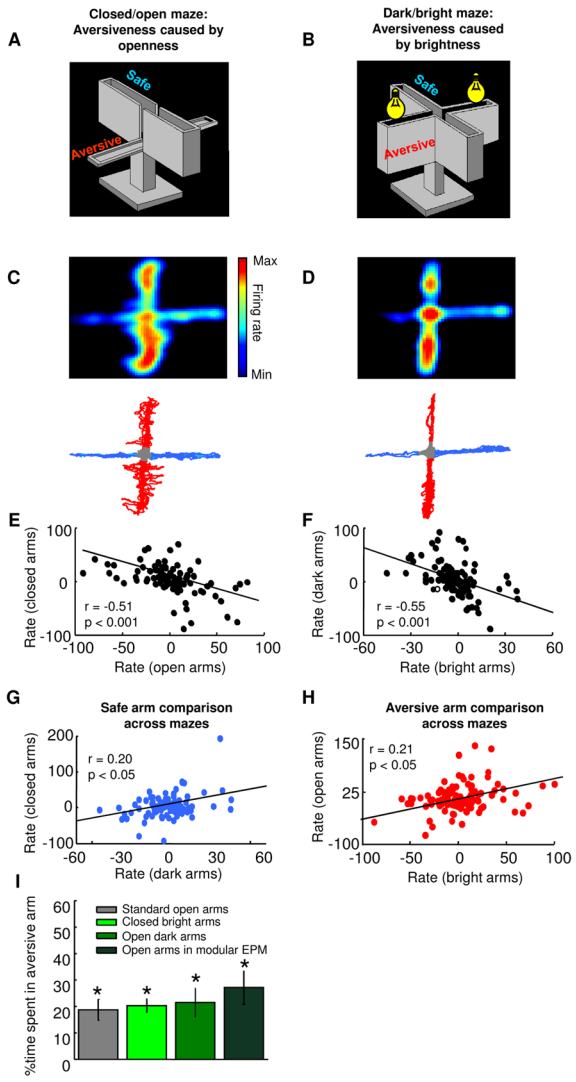

Figure 7. mPFC single units respond similarly to different aversive stimuli

(A) Standard EPM in the dark. Light level was <5 lux. (B) EPM with four closed arms. Two of the arms were illuminated with bright (600 lux) light. Light in the other arms remained < 5 lux. (C) Upper panel: spatial firing rate map of a representative single unit recorded in the standard EPM in the dark. Lower panel: Behavior track of the session from which this recording was obtained. Safe (closed) and aversive (open) arms are depicted in blue and red, respectively. (D) Upper panel: spatial firing map of the same unit shown in (C), but recorded in dark/bright maze. Note that the example unit fires preferentially in the aversive arms of both mazes. Lower panel: Behavior track of the session of the recording shown in the upper panel. Safe (dark) and aversive (bright) arms are depicted in blue and red, respectively. (E) Scatter plot showing that firing rates across closed and open arms were negatively correlated (maze shown in (A), n=105 units). (F) Scatter plot showing that normalized firing rates in the dark and bright arms were negatively correlated (maze shown in (B), n=105 units). (G–H) Correlations of normalized firing rates across the two mazes for safe arms (G) and aversive arms (n = 105 units) (H). Note that rates for arms of the same type were positively correlated even across mazes in which the aversive stimuli were different. (I) Bar graph showing the % time spent in the aversive arms in the standard and modified EPMs. In all

configurations of the EPM naive mice spent less than 50% time in the aversive arm (*$p<0.05$, Wilcoxon's signrank test). See also Figure S5.

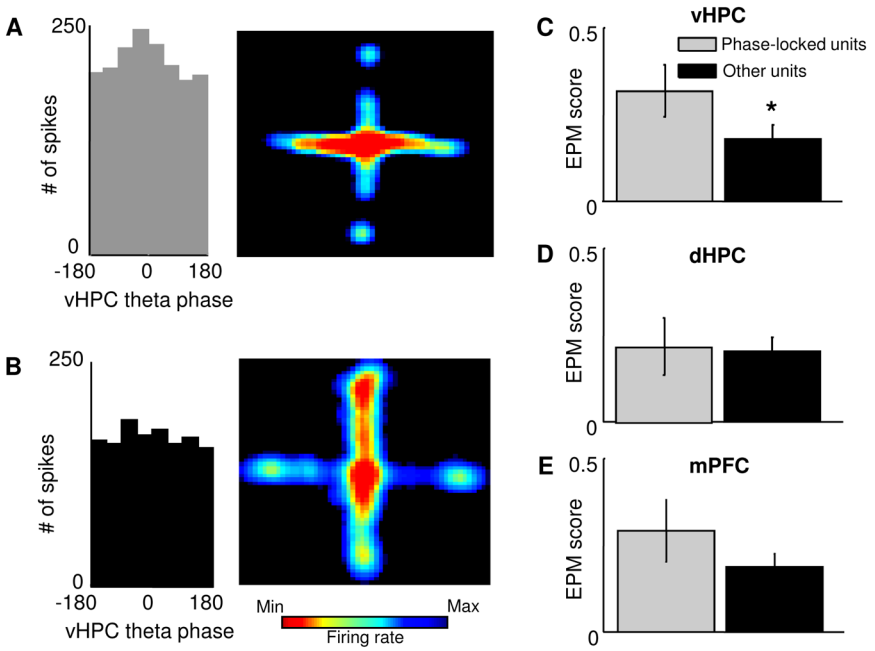

Figure 8. mPFC units phase-locked to vHPC theta oscillations have stronger task-related firing

(A,B) Left Panel: Distribution of the phases of firing relative to vHPC theta oscillations for an example mPFC single unit. This unit is significantly phase-locked to vHPC theta oscillations ($p<0.05$, Rayleigh's test for circular uniformity). Right panel: Spatial firing rate map for the same unit. Note that this unit is preferentially active in the open arms. (B) Same as (A), but for a unit that is not significantly phase-locked to vHPC theta (left panel) and that does not distinguish robustly closed arms from open arms (right panel). (C) Left panel: bar graph showing mean EPM scores for units that were (black bars) and were not (grey bars) significantly phase-locked to vHPC theta oscillations. Phase locked units had on average higher EPM scores than other units (mean score = 0.31 ± 0.07 and 0.17 ± 0.04, for phase locked and other units, respectively, $p<0.05$, Wilcoxon's test, $n = 69$ units) Right panel: normalized cumulative sum distributions of the EPM scores shown averaged in the left panel. Note that the difference seen in the left panel between the EPM score distributions of vHPC phase locked units and other units is not due to a change in the size of the right tail of the distribution. (D) and (E) Same as (C), but for phase locking to dHPC and mPFC theta oscillations. Phase-locking to dHPC or mPFC theta oscillations did not have significant effects on EPM scores ($p = 0.31$ and 0.07, respectively). See also Figure S2.

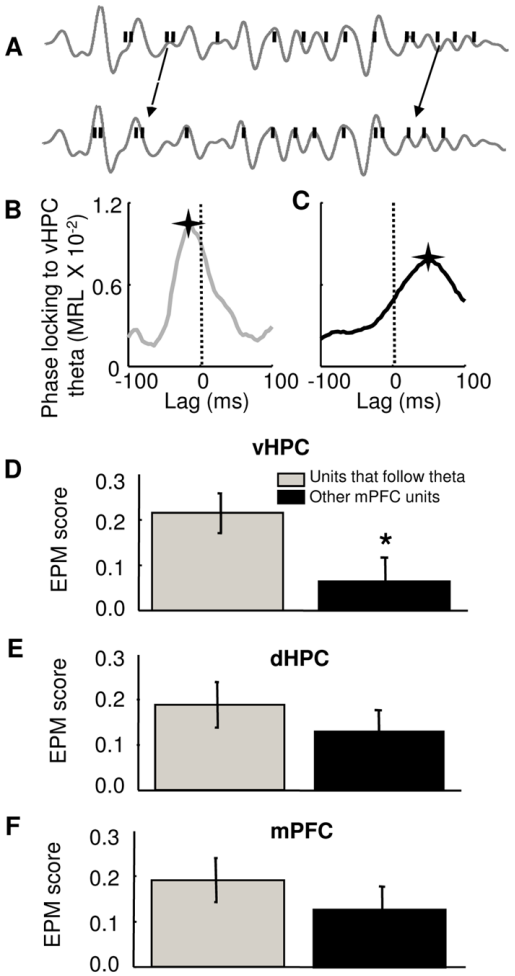

Figure 9. mPFC units that follow vHPC theta oscillations have more robust task-related firing patterns

(A) Shifting the spike train (black bars) backwards in time (lower panel) relative to the theta-filtered vHPC local field potential (grey lines) reveals stronger phase-locking. (B) and (C) Effect of shifting the spike train of two representative mPFC single units on the strength of phase-locking (MRL) to vHPC theta oscillations. The unit in (B) follows vHPC theta, as the maximal MRL value is observed at a negative lag (−12 ms), while the unit in (C) leads vHPC theta, with a peak at a positive lag (+54 ms). A star marks the position of the maximum MRL. A dashed line was plotted at zero lag for reference. (D) Left panel: bar graph showing mean +/− EPM scores for units with negative lags relative to hippocampal theta (grey) and all other units (black). Units that followed vHPC theta had significantly higher EPM scores (mean score = 0.24 ± 0.047 and 0.07 ± 0.05 for units that follow vHPC theta and other units, respectively. *$p<0.05$, Wilcoxon's test, n = 69 units). Right panel: normalized cumulative sum distributions of the EPM scores shown averaged in the left panel. (E) and (F) Same as (D), but for dHPC and mPFC theta oscillations. Units that followed mPFC or dHPC theta oscillations did not have higher EPM scores than other units, p=0.08 and 0.51, respectively).

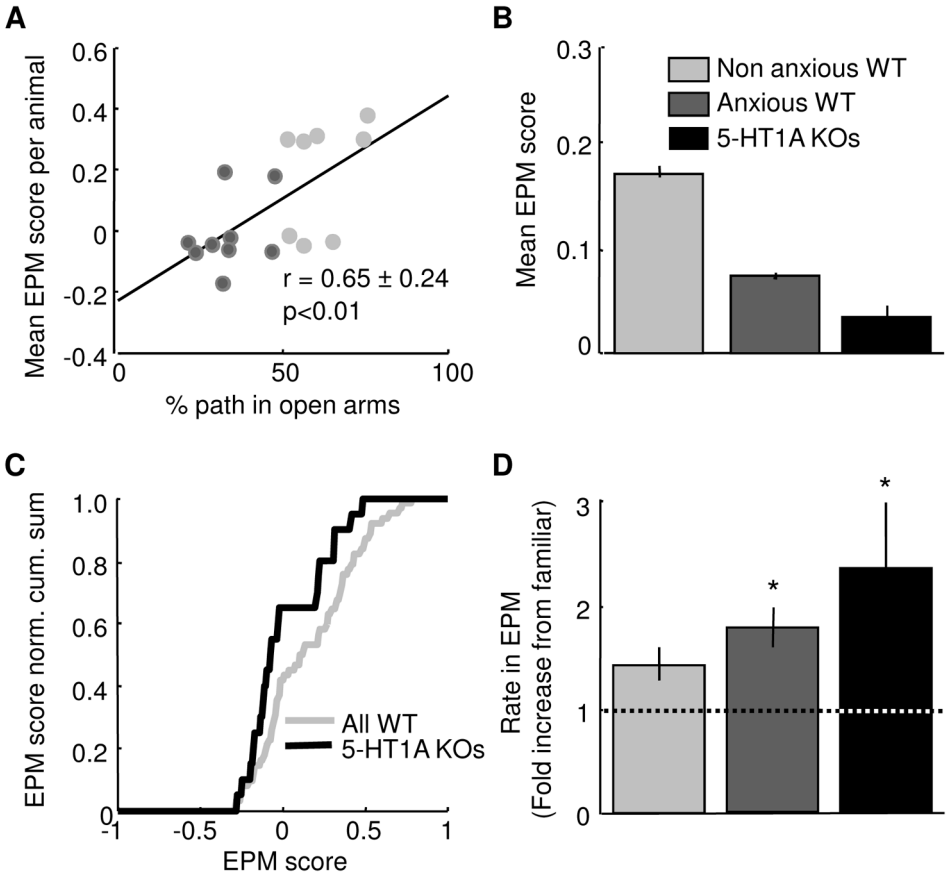

Figure 10. EPM scores and mPFC single unit activity are correlated with anxiety-related behavioral measures in the EPM

(A) Scatter plot of mean EPM score against % path in the open arms of the EPM for all animals with at least 3 simultaneously recorded single units with more than 100 spikes. EPM scores and open arm exploration are strongly positively correlated (r=+0.65, p<0.01). Animals were divided into two groups: those that were below (avoidant, n=9) and above (non-avoidant, n=8) 50 % path in the open arms. (B) Mean EPM scores for non-avoidant WT (mean score=0.171 ± 0.0051, n=61), avoidant WT (0.072 ± 0.0031, n= 95) and 5-HT1A receptor knockout mice (0.032 ± 0.011, n=20). (A–B) Units from WT mice recorded in the standard EPM at 200 and 0–5 Lux were pooled (n=39 units from the standard EPM at 200 Lux and n=117 units from the standard EPM in the dark). (C) EPM score normalized cumulative sum distributions for all WT single and all 5-HT1A receptor knockout single units. The two distributions are significantly different (p<0.05, Wilcoxon's test). (D) Bar graph showing mean rate in the EPM for non-avoidant WT, avoidant WT and 5HT-1A receptor knockout mice. Rates are plotted as fold increase from the familiar environment. No change (fold increase of 1) is plotted as a dotted line. Avoidant WT and 5-HT1A receptor knockout mice had significant increases in firing rate relative to the familiar environment in the EPM (*p<0.05). (C–D) As 5-HT1A knockout mice were only exposed to the EPM at 200 Lux, only WT sessions used at this illumination were used to make comparisons across genotypes (n=69 and 24 units for WT and knockout mice, respectively). See also Figure S3.